J Fusion Energ
DOI 10.1007/s10894-012-9537-1

ORIGINAL RESEARCH

Scaling Laws of Nitrogen Soft X-ray Yields from 1 to 200 kJ Plasma Focus

M. Akel · S. Lee

Abstract Numerical experiments are carried out systematically to determine the nitrogen soft X-ray yield for optimized nitrogen plasma focus with storage energy E_0 from 1 to 200 kJ. Scaling laws on nitrogen soft X-ray yield, in terms of storage energies E_0, peak discharge current I_{peak} and focus pinch current I_{pinch} were found. It was found that the nitrogen X-ray yields scales on average with $Y_{sxr,N} = 1.93 \times E_0^{1.21}$J ($E_0$ in kJ) with the scaling showing gradual deterioration as E_0 rises over the range. A more robust scaling is $Y_{sxr} = 8 \times 10^{-8} I_{pinch}^{3.38}$. The optimum nitrogen soft X-ray yield emitted from plasma focus is found to be about 1 kJ for storage energy of 200 kJ. This indicates that nitrogen plasma focus is a good water-window soft X-ray source when properly designed.

Keywords Plasma focus · Soft X-ray · Nitrogen gas · Lee model code

Introduction

Plasma focus devices with nitrogen filling gas has been used widely in plasma focus devices as an emitter of soft and hard X-rays [1–8], and plasma focus devices operated with pure nitrogen are developed as sources for X-ray microscopy [9–11]. X-ray microscopy allows the imaging of living hydrated biological specimens. The wavelength range between the K-absorption edges of oxygen ($\lambda = 2.34$ nm) and carbon ($\lambda = 4.38$ nm) is especially interesting for this because the radiation in this wavelength range (so called "water window") is weakly absorbed by water but strongly absorbed by organic matter resulting in a good contrast of wet samples [9]. Whilst many recent experiments have concentrated efforts on low energy devices [12–14] with a view of operating these as repetitively pulsed sources, other experiments have looked at X-ray pulses from larger plasma focus devices [15, 16] extending to the mega joule regime. However, numerical experiments simulating X-ray pulses from plasma focus devices are gaining more interest in the public domain. For example, the Institute of Plasma Focus Studies [17] conducted an International Internet Workshop on Plasma Focus Numerical Experiments [18], at which it was demonstrated that the Lee model code [19] not only computes realistic focus pinch parameters, but also absolute values of SXR yield Y_{sxr} which are consistent with those measured experimentally. A comparison was made for the case of the NX2 machine [14], showing good agreement between computed and measured Y_{sxr} as a function of operational pressure p_0 [18, 20]. This gives confidence that the Lee model code produces realistic results in the computation of Y_{sxr}.

Numerical experiments using Lee model have been carried out systematically to derive scaling laws on the neon [21, 22] and argon [23] soft X-ray yields, in terms of storage energies E_0, peak discharge current I_{peak} and focus pinch current I_{pinch} obtained from studies carried out over storage energies E_0 varying from 1 kJ^{-1} MJ for optimized plasma focus device parameters.

M. Akel (✉)
Department of Physics, Atomic Energy Commission,
P. O. Box 6091, Damascus, Syria
e-mail: pscientific@aec.org.sy

S. Lee
Institute for Plasma Focus Studies, 32 Oakpark Drive,
Chadstone, VIC 3148, Australia

S. Lee
INTI International University, 71800 Nilai, Malaysia

Published online: 30 March 2012

The Lee model code has been modified to include nitrogen gas and it has been then used to characterize the plasma focus device operated in nitrogen [24]. The suitable temperature range for generating H-like (Ly_α (1s-2p, N_2: 2.478 nm)) and He-like (He_β($1s^2$-1s3p, N_2: 2.496 nm)) ions in nitrogen plasma (therefore X-ray emissions in the water window region) was found to be between 74 and 173 eV (0.86×10^6–2×10^6 K) [17, 24].

Numerical experiments on low energy plasma focus with nitrogen filling gas using the latest version of Lee model [24, 25] have shown that the optimum nitrogen soft X-ray yield is about 0.064 J, which it is expected to increase with reducing the external inductance to maximum value of near 4 J at an achievable $L_0 = 15$ nH.

In the context of soft X-ray nitrogen scaling law over any significant range of energies, no experimental or numerical work appears to have been reported in the literature. In this paper, we show the comprehensive range of numerical experiments conducted to derive scaling laws on nitrogen soft X-ray yield, in terms of storage energies E_0, peak discharge current I_{peak} and focus pinch current I_{pinch} obtained from studies carried out over storage energies E_0 varying from 1 to 200 kJ for optimized plasma focus device parameters.

Numerical Experiments on Nitrogen Plasma Focus

The Lee Model code [19] has been used to carry out a series of numerical experiments over the energy range 1–200 kJ. In the code, nitrogen line radiation Q_L is calculated as follows:

$$\frac{dQ_L}{dt} = -4.6 \times 10^{-31} N_i^2 Z_{eff} Z_n^4 (\pi a_{min}^2) Z_{max}/T$$

Hence the SXR energy generated within the plasma pinch depends on the following properties: number density N_i, effective charge number Z_{eff}, atomic number of gas Z_n, pinch radius a_{min}, pinch length Z_{max}, plasma temperature T and the pinch duration. This generated energy is then reduced by the plasma self-absorption which depends primarily on density and temperature; the reduced quantity of energy is then emitted as the soft X-ray yield. In the modified Lee model code version RADPF5.15K, we take the nitrogen soft X-ray yield to be equivalent to line radiation yield i.e. $Y_{sxr} = Q_L$ at the following temperature range 74–173 eV (0.86×10^6–2×10^6 K). In any shot, for the duration of the focus pinch, whenever the focus pinch temperature is within this range, the line radiation is counted as nitrogen soft X-rays. Whenever the pinch temperature is outside this range, the line radiation is not included as nitrogen soft X-rays.

During all our numerical experiments, the following parameters are kept constant: the ratio b = c/a (1.5) the operating voltage V_0 (20 kV), the static inductance (30 nH), the ratio of stray resistance to surge impedance RESF (kept at 0.1). The model parameters f_m, f_c, f_{mr}, f_{cr} are also kept at fixed suitable values of 0.06, 0.7, 0.15 and 0.7, respectively.

The storage energy E_0 is changed (from 1 to 200 kJ) by changing the capacitance C_0 (from 5 μF up to 1,000 μF). Parameters that are varied are anode length z_0 and anode radius 'a', operating pressure p_0. Parametric variation at each E_0 follows the anode length z_0 and 'a' until all realistic combinations of E_0, z_0 and 'a' are investigated. In other words at each E_0, a p_0 is fixed, a z_0 is chosen and 'a' is varied until the largest Y_{sxr} is found. Then keeping the same values of E_0, another p_0 is selected. The procedure for parametric variation of z_0 and 'a' as described above is then carried out for this E_0 and new p_0 until the optimum combination of z_0 and 'a' is found. This procedure is repeated until for a fixed value of E_0, the optimum combination of p_0, z_0 and 'a' is found. The procedure is then repeated with a new value of E_0 [21–23].

Results and Discussion

After systematically carrying many numerical experiments using Lee model on nitrogen plasma focus following the above mentioned procedures, the optimized shots for various energies are tabulated in Table 1. This table shows optimized configuration found for each E_0 for 30 nH. From the data of Table 1, we plot Y_{sxr} against E_0 as shown in Fig. 1. From Fig. 1 we found that Y_{sxr} scales on average as $Y_{sxr,N} = 1.93 \times E_0^{1.21}$ at energies in the 1–200 kJ regions. We then plot Y_{sxr} against I_{peak} and I_{pinch} and obtain Fig. 2, which shows that $Y_{sxr} = 8 \times 10^{-8} I_{pinch}^{3.38}$ and $Y_{sxr} = 2 \times 10^{-7} I_{peak}^{2.97}$ (Ipeak and Ipinch in kA and Y_{sxr} in J). The resulting Y_{sxr} vs I_{pinch} and I_{peak} log–log curves found to be with the scaling index 3.4 and 3, respectively (Fig. 2). From Fig. 2 it can be seen that the resulting Y_{sxr} vs I_{peak} log–log curve has a larger scatter from linearity than Y_{sxr} vs I_{pinch} log–log curve. Another way of looking at the comparison of the I_{pinch} scaling and the I_{peak} scaling is to consider some unoptimised cases e.g. at very high or very low pressures. In these cases, Y_{sxr} is zero and I_{pinch} is zero but there is a value for I_{peak}. This is an argument that the I_{pinch} scaling is more robust. However it must be noted that both scaling are applicable only to optimized points. Nevertheless noting that the $Y_{sxr} \sim I_{pinch}$ scaling has less scatter than the $Y_{sxr} \sim I_{peak}$ scaling, the conclusion is that the I_{pinch} scaling is the more universal and robust one. Table 1 shows that the electrode geometry increases with

Table 1 Optimized configuration found for each E_0. Optimization carried out with RESF = 0.1, c = 1.5, L_0 = 30 nH and V_0 = 20 kV and model parameters f_m, f_c, f_{mr}, f_{cr} are fixed at 0.06, 0.7, 0.15 and 0.7, respectively, nitrogen gas

E_0 (kJ)	C_0 (μF)	a (cm)	z_0 (cm)	p_0 (Torr)	I_{peak} (kA)	I_{pinch} (kA)	v_a (cm/μs)	v_s (cm/μs)	v_p (cm/μs)	Y_{sxr} (J)	$I_{peak/a}$ (kA/cm)	Effi. (%)
1	5	1.3	1.0	4	222.2	140.8	4.8	15.0	10.9	1.5	170.9	0.15
2	10	1.6	2.0	4	312.1	190.9	5.9	16.4	11.9	4.2	195.1	0.21
6	30	2.4	4.0	4	516.2	297.9	6.6	17.2	12.4	19.3	215.1	0.32
10	50	2.9	5.0	4	638.7	359.5	6.8	17.2	12.4	36.4	220.2	0.36
20	100	3.6	12.0	4	889.9	464.0	8.2	18.1	13.1	85.5	247.2	0.43
40	200	4.5	15.0	4	1,154.7	590.3	8.4	18.6	13.3	194.0	256.6	0.48
80	400	5.5	25.0	4	1,475.0	734.4	9.0	19.0	13.6	404.7	268.2	0.51
120	600	6.0	33.0	4	1,661.2	828.2	9.4	19.6	14.0	590.3	276.9	0.49
160	800	6.5	40.0	4	1,807.1	897.2	9.5	19.6	14.0	777.9	278.0	0.49
200	1,000	7.0	43.0	4	1,930.6	950.7	9.4	19.4	13.9	967.3	275.8	0.48

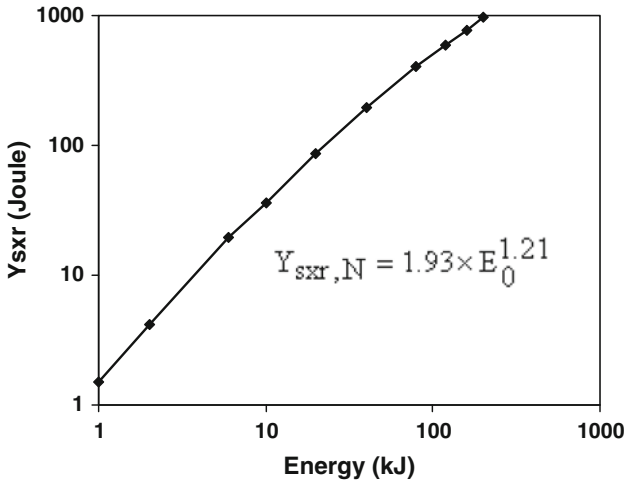

Fig. 1 Soft X-ray yields from nitrogen plasma focus versus storage energy with RESF = 0.1, c = 1.5, L_0 = 30 nH and V_0 = 20 kV and model parameters f_m, f_c, f_{mr}, f_{cr} are fixed at 0.06, 0.7, 0.15 and 0.7, respectively, nitrogen gas

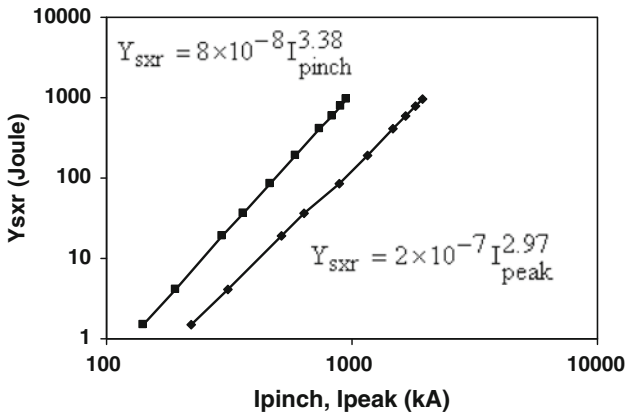

Fig. 2 Soft X-ray yields from nitrogen plasma focus versus I_{pinch}, I_{peak}

increasing the storage energy from 1 to 200 kJ, while it is noticed that the peak axial speed (v_a) suitable for maximum nitrogen soft X-ray yield changes over this wide energy range, this means that there is a required range of axial speed in plasma focus devices for nitrogen soft X-ray emission, for example, in our case these values are in the range 5–9.5 cm/μs (with an average value of 7.8 cm/μs). It can be also noticed, from this table, that the peak radial shock (v_s) and the peak radial piston speeds (v_p) over this wide energy range are slightly varying, and its average values are found to be v_s = 18 cm/μs, v_p = 13 cm/μs. The observations of the numerical experiments, bolstered by fundamental considerations is that the I_{pinch} scaling is the more universal and robust one. This implies that for applications requiring high X-ray yield, the plasma focus must be designed to optimize I_{pinch}. For example from Table 1, it can be seen that the optimum efficiency for SXR yield (0.51 %) is with capacitor bank energy of 80 kJ. One factor may be that beyond these optimum energies, I_{pinch} do not increase as well with bank energy due to the increasing dominance of the dynamic resistance of the axial phase in comparison with that of the bank impedance. Therefore for larger devices, it may be necessary to operate at a higher voltage and use higher driver impedance to have increased X-ray yield efficiency. So based on these numerical experiments, we can consider that the plasma focus operated with nitrogen gas as intense soft X-ray source in the water window region. Numerical experiments have been investigated [21–23], to determine the neon and argon soft X-ray yields for optimized plasma focus with storage energy E_0 from 1 to 1 MJ. Scaling laws on argon and neon soft X-ray yields, in terms of storage energies E_0, were found to be best averaged as: $Y_{sxr,Ar} = 0.07 \times E_0^{0.84}$ and $Y_{sxr,Ne} = 11 \times E_0^{1.2}$ (yield in J, E_0 in kJ), respectively at energies in the 2–400 kJ regions. By comparing our

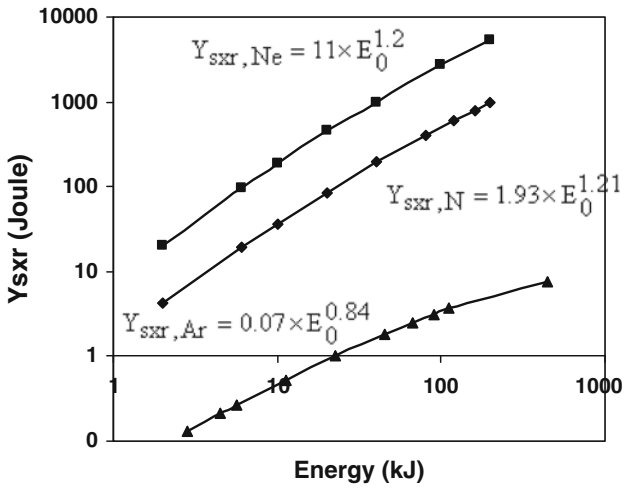

Fig. 3 Soft X-ray yields versus storage energy for neon, nitrogen and argon plasma focus

recent results for nitrogen plasma focus with argon and neon soft X-ray yields over this studied storage energy ranges, it is seen that the neon soft X-ray yield of plasma focus is the most intense one (Fig. 3). So considering all these numerical experiments, we find that the plasma focus is a powerful source of X-rays with wavelengths which may be suitably selected for microlithography, micromachining and microscopy simply by selecting the working gas (Neon or Argon or Nitrogen correspondingly) and choosing corresponding design and operating parameters of the device.

Conclusions

Numerical experiments are investigated on nitrogen plasma focus at different operational conditions. The optimum combination p_0, z_0 and 'a' is found for each E_0 within the range of 1–200 kJ. The results show that nitrogen X-ray yields scale on average with $Y_{sxr,N} = 1.93 \times E_0^{1.21}$ over 1–200 kJ regions (yields in joules and storage energy in kJ). These numerical experiments confirm that the Y_{sxr} vs I_{pinch} scaling is more robust and universal, and scale well with $Y_{sxr} = 8 \times 10^{-8} I_{pinch}^{3.38}$ (yields in J and current in kA). This implies that for applications requiring high X-ray yield in the water window region, the key is to optimize I_{pinch}. The optimum nitrogen soft X-ray yield efficiency is found to be 0.51 % at energy of 80 kJ with yields close to 0.5 % in the range 40–200 kJ.

Acknowledgments The authors would like to thank Director General of AECS, for encouragement and permanent support. They would also like to express many thanks to Mrs. Sheren Isamael, who collaborated going through all the numerical experiments using Lee Model.

References

1. M. Shafiq et al., Mod. Phys. Lett. B **16**(9), 309 (2002)
2. M. Shafiq et al., J. Fusion Energ. **20**(3), 113 (2001) (q 2002)
3. N.K. Neog et al., J. Appl. Phys. **99**, 013302 (2006)
4. A. Roomi et al., J. Fusion Energ. (2011). doi: 10.1007/s10894-011-9395-2
5. M. A. I. Elgarhy, M. Sc. thesis, Plasma focus and its applications, Cairo (2010)
6. A. Roomi et al., J. Fusion Energ. (2011). doi:10.1007/s10894-011-9388-1
7. A. Roomi et al., J. Fusion Energ. (2011). doi:10.1007/s10894-011-9464-6
8. A. Roomi et al., J. Fusion Energ. (2011). doi:10.1007/s10894-011-9501-5
9. R. Lebert, D. Rothweiler, A. Engel, K. Bergmann, W. Neff, Opt. Quantum Electron **28**, 241–259 (1996)
10. F. Richer et al., *Dense z-pinches*. Second International Conference (New York, AIP, 1989) (AIP Conference Proceedings 195)
11. R. Lebert, A. Engel, W. Neff, J. Appl. Phys. **78**(11), 6414–6420 (1995)
12. Y. Kato, S.H. Be, Appl. Phys. Lett. **48**, 686 (1986)
13. E.P. Bogolyubov et al., Phys. Scr. **57**, 488–494 (1998)
14. S. Lee et al., IEEE Trans. Plasma Sci. **26**, 1119 (1998)
15. N.V. Filippov et al., IEEE Trans. Plasma Sci. **24**, 1215–1223 (1996)
16. N.V. Filippov et al., Phys. Lett. A **211**, 168–171 (1996)
17. Institute for Plasma Focus Studies. http://www.plasmafocus.net
18. Internet Workshop on Plasma Focus Numerical Experiments (IPFS-IBC1), 14 April–19 May (2008)
19. S. Lee, *Radiative Dense Plasma Focus Computation Package: RADPF*. http://www.plasmafocus.net, http://www.intimal.edu.my (2011)
20. S. Lee et al., J. Appl. Phys. **106**, 023309 (2009)
21. S. Lee et al., Plasma Phys. Control. Fusion **51**, 105013 (2009)
22. S.H. Saw, S. Lee, Energ. Power Eng. **2**(1), 65–72 (2010)
23. M. Akel, S. Lee, J. Fusion Energ. **31**(2), 143–150 (2012)
24. M. Akel, Sh Al-Hawat, S. Lee, J. Fusion Energ. **28**(4), 355–363 (2009)
25. M. Akel, Sh Al-Hawat, S. Lee, J. Fusion Energ. **29**(1), 94–99 (2010)